

Activation of *RET* as a Dominant Transforming Gene by Germline Mutations of *MEN2A* and *MEN2B*

Massimo Santoro, Francesca Carlomagno, Alfredo Romano, Donald P. Bottaro, Nina A. Dathan, Michele Grieco, Alfredo Fusco, Giancarlo Vecchio, Brona Matošková, Matthias H. Kraus, Pier Paolo Di Fiore*

Multiple endocrine neoplasia types 2A and 2B (*MEN2A* and *MEN2B*) and familial medullary thyroid carcinoma are dominantly inherited cancer syndromes. All three syndromes are associated with mutations in *RET*, which encodes a receptor-like tyrosine kinase. The altered *RET* alleles were shown to be transforming genes in NIH 3T3 cells as a consequence of constitutive activation of the *RET* kinase. The *MEN2A* mutation resulted in *RET* dimerization at steady state, whereas the *MEN2B* mutation altered *RET* catalytic properties both quantitatively and qualitatively. Oncogenic conversion of *RET* in these neoplastic syndromes establishes germline transmission of dominant transforming genes in human cancer.

MEN2A, **MEN2B**, and familial medullary thyroid carcinoma (FMTc) are dominantly inherited cancer syndromes. *MEN2A* is defined by the presence of medullary thyroid carcinoma, pheochromocytoma, and hyperparathyroidism. In addition to these abnormalities, *MEN2B* is characterized by skeletal abnormalities, ganglioneuromas of the intestinal tract, and mucosal neuromas. All three syndromes are associated with germline mutations of the *RET* proto-oncogene (1, 2), which codes for a receptor-like tyrosine kinase (3) whose ligand has not yet been identified. In the case of *MEN2A* and FMTc, point mutations result in the substitution of one of five Cys residues in the extracellular domain of *RET* (1). In *MEN2B*, a T→C transition in the tyrosine kinase domain causes a Met→Thr substitution at position 918 (2). It is not known how these alterations contribute to neoplasia. In the simplest model, the mutated *RET* allele acts as a dominant transforming gene. Alternatively, the mutations may inactivate a possible tumor suppressor function of proto-*RET*. In this scenario, the reduced dosage of proto-*RET* might be sufficient to

trigger transformation or the product of the mutated allele might inhibit the function of the wild-type protein, thus exerting a dominant negative function (4).

To test these possibilities, we engineered eukaryotic expression vectors (5) encoding proto-*RET* (LTR-*ret*), three different *MEN2A* alleles (*RET* Cys⁶³⁴→Tyr, Arg, or Trp; *MEN2AY*, *MEN2AR*, and *MEN2AW*, respectively), and the *MEN2B* allele (*RET* Met⁹¹⁸→Thr; *MEN2B*). After transfection in NIH 3T3 fibroblasts, *RET* mutants, but not proto-*RET*, displayed high transforming efficiency (Fig. 1). In addition, *MEN2A* and *MEN2B* transfectants displayed high clonogenic ability in soft agar, whereas proto-*RET* transfectants did not show growth (6).

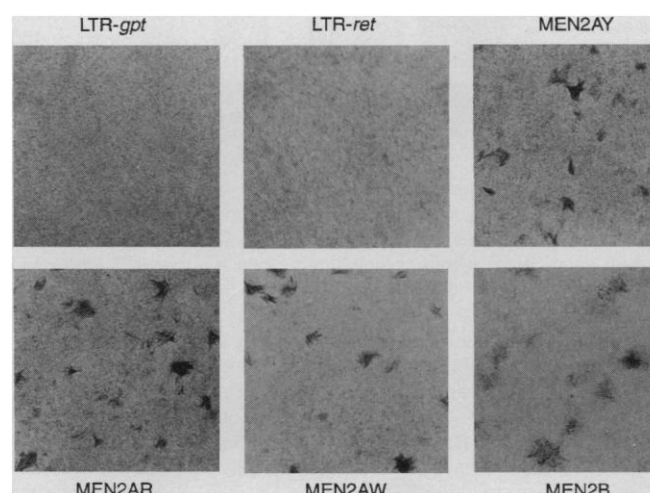
Mass populations of transfectants were obtained by killer HAT selection and used for protein analysis. *RET* was detected in two forms, one ~145 kD and the other

~160 kD (Fig. 2A), in all of the transfectants (7). Comparable amounts of *RET* were then immunoprecipitated from the various transfectants and assayed for phosphotyrosine (pTyr) content (8), a hallmark of receptor autophosphorylation and activation. No tyrosine phosphorylation of the proto-*RET* product was detectable, whereas *RET-MEN2A* and *RET-MEN2B* products showed high amounts of pTyr (Fig. 2A). Similar results were obtained in immunocomplex kinase assays (9). The proto-*RET* product displayed little, if any, kinase activity, whereas *RET-MEN2A* and *RET-MEN2B* became autophosphorylated (Fig. 2B). Autophosphorylation of *RET-MEN2B* was consistently one-third to one-fifth that of the *RET-MEN2A* forms in both assays (Fig. 2, A and B).

We analyzed a medullary thyroid carcinoma cell line, TT (10), by the reverse transcriptase polymerase chain reaction (RT-PCR) and by nucleotide sequencing and found that it expressed both a wild-type and a mutated *RET* allele (Cys⁶³⁴→Trp) (11). This cell line allowed us to validate our observations with NIH 3T3 cells in a setting representative of a naturally occurring neoplasm. For comparison, we used the neuroblastoma cell line SK-N-BE (10), which expresses only wild-type *RET* (11). In TT cells, *RET* displayed detectable pTyr amounts, whereas no pTyr was detectable in *RET* expressed by SK-N-BE cells (Fig. 2C). Similarly, *RET* from TT cells, but not from SK-N-BE cells, displayed autophosphorylation activity in vitro (Fig. 2D).

To investigate the mechanism of activation of the mutated *RET* alleles, we analyzed *RET-MEN2A* and *RET-MEN2B* by nonreducing SDS-polyacrylamide gel electrophoresis (SDS-PAGE). Under these conditions, *RET-MEN2B* migrated as monomeric forms at ~150 to 160 kD, whereas *RET-MEN2A* displayed an additional species at ~300 kD (Fig. 3A), consistent with

Fig. 1. Transforming activity of *RET* constructs after transfection in NIH 3T3 cells (18, 19). LTR-*gpt*, vector control. Transforming efficiencies expressed in focus-forming units per picomole of DNA were as follows: proto-*RET*, <1; *MEN2AY*, 6.9×10^3 ; *MEN2AR*, 3.5×10^3 ; *MEN2AW*, 1.5×10^3 ; and *MEN2B*, 3.7×10^3 . Efficiencies were corrected for marker selectable colony formation.



M. Santoro, F. Carlomagno, N. A. Dathan, M. Grieco, G. Vecchio, Centro di Endocrinologia ed Oncologia Sperimentale del Consiglio Nazionale delle Ricerche (CNR) e Dipartimento di Biologia e Patologia Cellulare e Molecolare "L. Califano," Università degli Studi, Napoli, Italy. A. Romano, Laboratory of Experimental Carcinogenesis, National Cancer Institute, National Institutes of Health (NIH), Bethesda, MD 20892, USA. D. P. Bottaro, M. H. Kraus, P. P. Di Fiore, Laboratory of Cellular and Molecular Biology, National Cancer Institute, NIH, Bethesda, MD 20892, USA.

A. Fusco, Dipartimento di Medicina Sperimentale e Clinica, Facoltà di Medicina e Chirurgia, Catanzaro, Italy. B. Matošková, Laboratory of Cellular Development and Oncology, National Institute of Dental Research, NIH, Bethesda, MD 20892, USA.

*To whom correspondence should be addressed.

the size of disulfide-linked homodimers. RET dimers were present in all of the MEN2A transfectants (Fig. 3B). In addition, the dimer contained at least 10 times more pTyr *in vivo* than the monomer (Fig. 3B), indicating that it is the form with constitutive kinase activity. We postulate that the Cys residues, disrupted by the MEN2A mutations, are normally involved in intramolecular disulfide bonds. The mutations may render the partner Cys available for aberrant disulfide bonding with other mutant RET molecules and thus create active homodimers. Such a mechanism has been described for *in vitro* mutagenized erythropoietin receptor and epidermal growth factor receptor (EGFR) (12).

In the case of RET-MEN2B, we did not detect RET dimers (Fig. 3A). To verify this, we performed *in vivo* cross-linking (13) experiments on MEN2B transfectants with 1-(3-dimethylaminopropyl)-3-ethylcarbodiimide hydrochloride (EDC). Under conditions in which other receptor homodimers, such as RET-MEN2A, EGFR, and an EGFR-RET chimera (14) were cross-linked, no RET-MEN2B dimers were detectable (15), suggesting that RET-MEN2B is activated by an intramolecular mechanism.

MEN2B is a clinically more complex and aggressive disease than MEN2A. However, the RET-MEN2B protein did not display increased kinase activity or transforming ability, as compared with RET-

MEN2A. Thus, the clinical differences between the two syndromes cannot be explained by an increased transforming ability of RET-MEN2B. We therefore tested the possibility that the MEN2B mutation alters the substrate specificity of RET. We first obtained maps of pTyr-containing tryptic peptides for RET-MEN2A and RET-MEN2B after autophosphorylation *in vitro* (Fig. 4A) (16). The RET-MEN2A map matched that obtained with an EGFR-RET chimera (14), which represents the closest "physiological" control of RET autophosphorylation in the absence of a RET ligand (Fig. 4A). RET-MEN2B displayed a different phosphopeptide map, indicating alter-

ations in its autocatalytic specificity (Fig. 4A). We then studied the two-dimensional electrophoretic pattern of RET-MEN2A and RET-MEN2B substrates in NIH 3T3 transfectants (17). Although there was similarity of substrate phosphorylation, several spots appeared differentially phosphorylated in RET-MEN2B and RET-MEN2A transfectants (Fig. 4B). These results show that the MEN2B mutation alters the substrate specificity of RET. We propose that the nature and availability of substrates in different cell types control RET activity at a postreceptor level, resulting, in the case of MEN2B, in an organ-specific growth advantage. This model is consistent with our

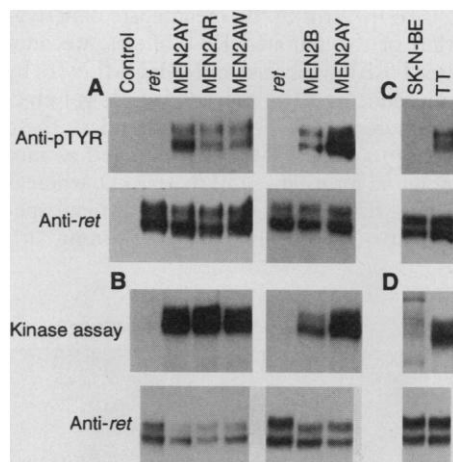


Fig. 2. Autophosphorylation of wild-type and mutant RET proteins *in vivo* and *in vitro*. Comparable amounts of RET proteins from the indicated cells were immunoprecipitated with a polyclonal antibody to RET (Anti-*ret*). The immunoprecipitates were then either immunoblotted with anti-*ret* (A through D, bottom panels) or a monoclonal antibody to phosphotyrosine (Anti-pTyr) (A and C, top panels) or subjected to an *in vitro* immunocomplex kinase assay (B and D, top panels) (9). (A and B) NIH 3T3 transfectants. Control, NIH 3T3 cells; *ret*, NIH-*proto-RET* cells. (C and D) TT and SK-N-BE cells.

Fig. 3. (A) Comparable amounts of RET proteins from the indicated transfectants were fractionated by SDS-PAGE under reducing or non-reducing conditions. Immunoblots were developed with anti-*ret* or anti-pTyr. Molecular size markers are indicated in kilodaltons; the positions of RET monomers and dimers are also indicated. (B) Covalent dimerization of RET in MEN2A transfectants. Immunoblot performed as in (A).

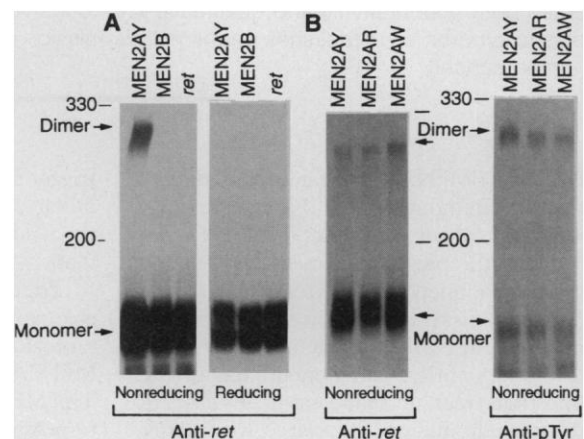
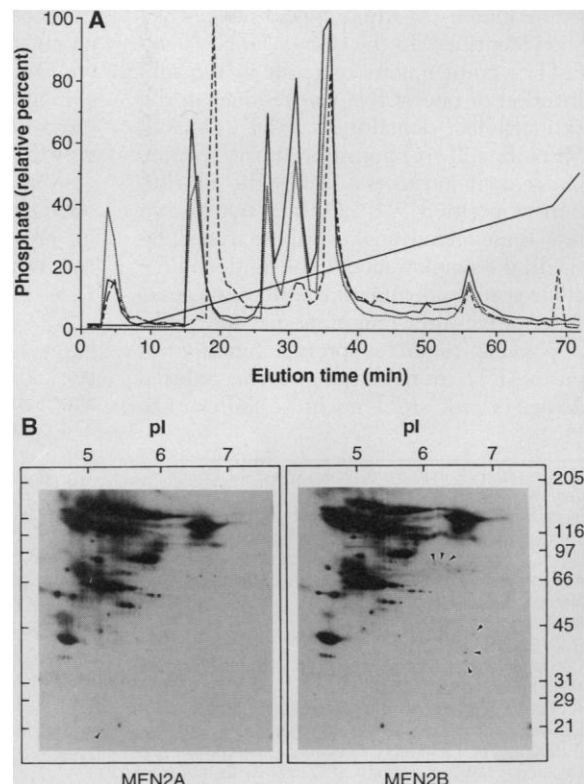


Fig. 4. Substrate specificity of wild-type and mutant RET proteins. (A) Tryptic phosphopeptide maps. An EGFR-RET chimera (dotted line), RET-MEN2AY (solid line), and RET-MEN2B (dashed line) were analyzed as in (16). The EGFR-RET chimera autophosphorylation reaction was carried out after *in vitro* stimulation with epidermal growth factor (4 μ g/ml). Results are expressed as a percentage of the counts per minute relative to the highest peak for each receptor. Maximum peaks were EGFR-RET, 4909 cpm; RET-MEN2A, 2666 cpm; and RET-MEN2B, 4738 cpm. The straight line depicts the acetonitrile gradient in percent (v/v). (B) Two-dimensional electrophoresis of pTyr-containing proteins. Lysates were prepared from serum-starved NIH 3T3 cells transfected with RET-MEN2AY (left) or RET-MEN2B (right). Immunoprecipitates with anti-pTyr (from 6 mg of total protein) were analyzed by two-dimensional electrophoresis as in (17). Immunoblots were developed with anti-pTyr. Molecular size markers are indicated on the right (in kilodaltons), and isoelectric points (pI's) are indicated at the top. Arrowheads identify spots differentially phosphorylated by RET-MEN2A and RET-MEN2B.



observation that the mitogenic potency of RET varies in different target cells (14).

These data establish that mutations in MEN2A and MEN2B convert RET into a dominant transforming gene. They also show the underlying mechanism to be a dominant oncogenic conversion rather than a loss of suppressor function. This finding is based on the observations that MEN2A and MEN2B mutations concomitantly activate the intrinsic kinase and transforming ability of RET and that mutant RET is enzymatically activated in the presence of a coexpressed normal allele as was shown in TT cells. Thus, the oncogenic conversion of RET illustrates that a dominant transforming gene can have a causal role in human hereditary neoplasia. In addition, our identification of the molecular mechanisms of RET activation provides the basis for therapeutic strategies in MEN2A, MEN2B, and FMTC.

REFERENCES AND NOTES

1. L. M. Mulligan *et al.*, *Nature* **363**, 458 (1993); L. M. Mulligan *et al.*, *Nat. Genet.* **6**, 70 (1994); H. Donis-Keller *et al.*, *Hum. Mol. Genet.* **2**, 851 (1993).
2. R. M. Hofstra *et al.*, *Nature* **367**, 375 (1994); K. M. Carlson *et al.*, *Proc. Natl. Acad. Sci. U.S.A.* **91**, 1579 (1994).
3. M. Takahashi *et al.*, *Oncogene* **3**, 571 (1988); M. Takahashi, Y. Buma, H. Hiai, *ibid.* **4**, 805 (1988).
4. R. A. Weinberg, *Science* **254**, 1138 (1991); A. G. Knudson, *Proc. Natl. Acad. Sci. U.S.A.* **90**, 10914 (1993).
5. We assembled the open reading frame (ORF) of proto-RET by starting from clones derived from an SK-N-BE complementary DNA (cDNA) library (corresponding to the extracellular portion of RET) and a fragment of a described EGFR-RET construct (14), corresponding to the intracellular portion of RET. We completely sequenced the resulting cDNA, which encodes the short isoform of the RET protein (3), on both strands and found it to match exactly the published sequence of wild-type RET (3). The proto-RET ORF was then cloned in the LTR-2 plasmid (18) to yield the LTR-ret eukaryotic expression vector. Using the RT-PCR, we cloned cDNA fragments with the desired mutations from RNA obtained from neoplastic tissues of individuals with MEN2A and MEN2B. Nucleotide sequence analysis confirmed that no other mutations were present in the cDNA fragments. For the MEN2A expression vectors, Nde I-Eco RI fragments [corresponding to positions 1717 to 2348 of the proto-RET sequence (3)] from the mutated cDNAs were individually substituted for the analogous fragment in LTR-ret. For the MEN2B expression vector, a Bgl II-Bcl I fragment (positions 2765 to 2972 of proto-RET) was substituted for the analogous fragment in LTR-ret. A second cycle of sequence analysis confirmed the introduction of the expected mutations. Because all of the mutations were introduced directly into the LTR-ret vector, all constructs were identical except for the specified mutations, thus allowing comparison of their transforming abilities.
6. M. Santoro, M. H. Kraus, P. P. Di Fiore, unpublished data.
7. M. Takahashi, Y. Buma, M. Taniguchi, *Oncogene* **6**, 297 (1991).
8. Immunoprecipitation and immunoblotting experiments were performed as in (14). Antibodies included a polyclonal antibody to RET (14) and the 4G10 monoclonal antibody to phosphotyrosine (Upstate Biotechnology, Lake Placid, NY). RET-MEN2A and RET-MEN2B were expressed at higher amounts than the proto-RET product (15-fold and 5-fold, respectively). These differences were due in part to

- higher amounts of transcripts (approximately three- to fivefold higher amounts of RET-specific mRNA in MEN2A and MEN2B transfectants, as compared with proto-RET transfectants) and in part to the increased half-life of the RET-MEN2A protein, as compared with RET-MEN2B (6 versus 3.5 hours, respectively) (M. Santoro and P. P. Di Fiore, unpublished data).
9. The immunocomplex kinase assay was performed as in (16). Wild-type and mutant RETs were immunoprecipitated with the antibody to RET (14). The final kinase mixture contained 0.1% Triton X-100, 20 mM Hepes (pH 7.5), 150 mM NaCl, 15 mM MgCl₂, 15 mM MnCl₂, and 20 μ Ci of γ -³²P-labeled adenosine triphosphate (3000 Ci/mmol). In the experiment shown, the reaction was for 20 min at room temperature. Similar results were obtained under initial conditions (1 min at 4°C).
 10. The TT and SK-N-BE cells were purchased from the American Type Culture Collection and grown in Dulbecco's modified Eagle's medium supplemented with 10% fetal calf serum.

11. M. Santoro, unpublished data.
12. S. S. Watowich *et al.*, *Proc. Natl. Acad. Sci. U.S.A.* **89**, 2140 (1992); A. Sorokin, M. A. Lemmon, A. Ulrich, J. Schlessinger, *J. Biol. Chem.* **269**, 9752 (1994).
13. C. Cochet *et al.*, *J. Biol. Chem.* **263**, 3290 (1988).
14. M. Santoro *et al.*, *Mol. Cell. Biol.* **14**, 663 (1994).
15. F. Carlomagno and P. P. Di Fiore, unpublished data.
16. O. Segatto *et al.*, *Mol. Cell. Biol.* **11**, 3191 (1991).
17. Two-dimensional electrophoretic analysis of immunoprecipitates of pTyr was performed as described [A. Romano *et al.*, *Oncogene* **9**, 2923 (1994)].
18. P. P. Di Fiore *et al.*, *Science* **237**, 178 (1987).
19. M. Wigler *et al.*, *Cell* **11**, 223 (1977).
20. Supported in part by grants from the Associazione Italiana Ricerca sul Cancro, the Progetto Finalizzato CNR-Applicazioni Cliniche della Ricerca Oncologica, and the Progetto Finalizzato CNR-Biotecnologia e Bistrumentazione.

13 July 1994; accepted 23 November 1994

A Hot Spot of Binding Energy in a Hormone-Receptor Interface

Tim Clackson* and James A. Wells†

The x-ray crystal structure of the complex between human growth hormone (hGH) and the extracellular domain of its first bound receptor (hGHbp) shows that about 30 side chains from each protein make contact. Individual replacement of contact residues in the hGHbp with alanine showed that a central hydrophobic region, dominated by two tryptophan residues, accounts for more than three-quarters of the binding free energy. This "functional epitope" is surrounded by less important contact residues that are generally hydrophilic and partially hydrated, so that the interface resembles a cross section through a globular protein. The functionally important residues on the hGHbp directly contact those on hGH. Thus, only a small and complementary set of contact residues maintains binding affinity, a property that may be general to protein-protein interfaces.

Specific protein-protein interactions are critical events in most biological processes. A number of crystallographic studies have shown that the binding interfaces between proteins are generally large (600 to 1300 Å²) and include many intermolecular contacts, involving 10 to 30 side chains from each protein (1–3). However, structural analysis alone cannot show whether all of these contacts are important for tight binding. A complete understanding of the chemistry of protein-protein association also requires a functional map of each binding surface, to reveal to what extent each contact contributes to the overall free energy of binding.

The initial event in signaling through the hGH receptor is the binding of the extracellular domain (hGHbp) to site 1 of hGH to form a high-affinity 1:1 complex (dissociation constant, K_d , of 0.3 nM, corresponding to a binding free energy, ΔG , of -12.3 kcal/mol) (4, 5). The crystal structure of this

complex (3, 6) shows that on each protein a surface area of about 1300 Å² becomes buried (defined by calculated inaccessibility to solvent) (7), including 33 side chains on the receptor (Fig. 1A). We mutated each of these side chains individually to alanine, except for G168 and the C108–C122 disulfide (8). Substitution by alanine deletes all interactions made by atoms beyond the β carbon and should reveal the contribution to binding energy made by the removed portion of the side chain (9). Each mutant hGHbp was expressed in *Escherichia coli*, purified to >90% homogeneity, and assayed for hGH binding affinity (10, 11).

Fewer than half of the mutations caused substantial loss in binding affinity (Fig. 1B). By far the greatest reductions in affinity (>4.5 kcal/mol) occurred on substituting two tryptophan residues, W104 and W169 (12). Large effects (1.5 to 3.5 kcal/mol) were also seen for alanine substitutions at other hydrophobic residues (I103, I105, P106, and I165), and generally smaller effects (1 to 2 kcal/mol) were seen for some charged residues (R43, E44, D126, E127, and D164). This subset of 11 contact residues, which we term the functional epitope, maps to a con-

Department of Protein Engineering, Genentech, 460 Point San Bruno Boulevard, South San Francisco, CA 94080, USA.

*Present address: ARIAD Pharmaceuticals, 26 Lansdowne Street, Cambridge, MA 02139, USA.

†To whom correspondence should be addressed.